ATLAS PUBLIC NOTE

August 19, 2009

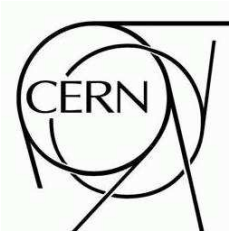

ATLAS Sensitivity to the Standard Model Higgs in the HW and HZ Channels at High Transverse Momenta

ATLAS Collaboration

Abstract

Until recently it was thought that for Higgs boson searches at the Large Hadron Collider, WH and ZH production where the Higgs boson decays to $b\bar{b}$ would be poor search channels due to large backgrounds. Recent phenomenological studies have indicated that at high transverse momenta, employing state-of-the-art jet reconstruction and decomposition techniques, these processes can be recovered as promising search channels for the Standard Model Higgs boson around 120 GeV in mass. We investigate this claim using a realistic simulation of the ATLAS detector.

ATL-PHYS-PUB-2009-088
20 August 2009

1 Introduction

A key aim of the LHC is to elucidate the Standard Model mechanism of mass generation, and hence electroweak symmetry breaking, either by discovering the Higgs boson or by proving that it does not exist. Current electroweak fits, together with the LEP and Tevatron exclusion limits, favour a light Higgs boson, i.e. one around 120 GeV in mass [1]. This mass region is particularly challenging both at the LHC and at the Tevatron, and any SM Higgs-boson discovery is expected to rely on a combination of several search channels, including $gg \to H \to \gamma\gamma$, $qqH \to qq\tau\tau$, $qqH \to qqWW$ and the associated production with $t\bar{t}$ pairs [2].

Two significant channels that have generally been considered less promising are those of Higgs-boson production in association with a vector boson, $pp \to WH$ or ZH, followed by the dominant light Higgs boson decay, to two b-jets. Reconstructing W or Z associated $H \to b\bar{b}$ production would typically involve identifying a leptonically decaying vector boson, plus two jets tagged as containing b-hadrons. Identification is difficult due to large backgrounds and low signal acceptance.

A recent study [3] argued that focusing analysis on VH (where V is a W or Z) production in a boosted regime, in which both bosons have large transverse momenta and are back-to-back, has significant advantages over a more inclusive search. This region corresponds to only a small fraction of the total VH cross-section (about 5% for $p_{\mathrm{T}} > 200\,\mathrm{GeV}$), but kinematic acceptance is larger, while the backgrounds are reduced.

The use of jet-finding and b-tagging geared to identifying the characteristic structure of a fast-moving Higgs boson that decays to b and $\bar{b}$ in a common neighbourhood in angle is a key element of the analysis. Related sub-jet analysis techniques using the $k_\perp$ algorithm [4, 5] to identify boosted hadronically decaying W bosons in vector-boson scattering events [6] have been shown to be viable [2, 7, 8] with the ATLAS detector [9]. However, there are several new features involved in the Higgs analysis, notably the use of the Cambridge/Aachen (C/A) jet algorithm [10, 11] and the stringent requirement on double b-tagging within a single jet. A detailed evaluation of the capability of ATLAS in this channel is required, and is the purpose of this note.

The analysis is performed in three subchannels based upon the decay of the vector boson.

(a) Missing transverse momentum $E_{\mathrm{T}}^{\mathrm{miss}} > 30\,\mathrm{GeV}$ plus a lepton (e or μ) with $p_{\mathrm{T}} > 30\,\mathrm{GeV}$, consistent with a W boson with $p_{\mathrm{T}} > \hat{p}_T^{\mathrm{min}}$,

(b) An e^+e^- or $\mu^+\mu^-$ pair with an invariant mass $80 < m < 100\,\mathrm{GeV}$ and $p_{\mathrm{T}} > \hat{p}_T^{\mathrm{min}}$,

(c) $E_{\mathrm{T}}^{\mathrm{miss}} > \hat{p}_T^{\mathrm{min}}$.

The sample from selection (a) is dominated by $HW, W \to \mu\nu, e\nu$, sample (b) contains the $HZ, Z \to e^+e^-/\mu^+\mu^-$ signal, and sample (c) contains a mixture of $HZ, Z \to \nu\bar{\nu}$ and HW where a lepton from the W is outside the acceptance. The vector boson decays to τ leptons are not explicitly searched for but contribute to some extent to samples (a) and (c): in the case of the $l\nu b\bar{b}$ channel, the $W \to \tau\nu$ decay mode contributes to ≈ 9 % of the signal.

Sample selection (b) is rather clean but has a low cross-section. Selections (a) and (c) have higher signal cross-sections but are more vulnerable to background from $t\bar{t}$ production. A value of $\hat{p}_T^{\mathrm{min}}$ of 200 GeV has been chosen.

The note is structured as follows. First we describe the simulation samples used. Then Section 3 gives some detail on the more novel aspects of the analysis (subjet analysis and b-tagging) used in identifying Higgs candidates. Section 4 describes the complete analysis, including the trigger and event selection, and in Section 5 we make an estimate of the potential significance of this channel.

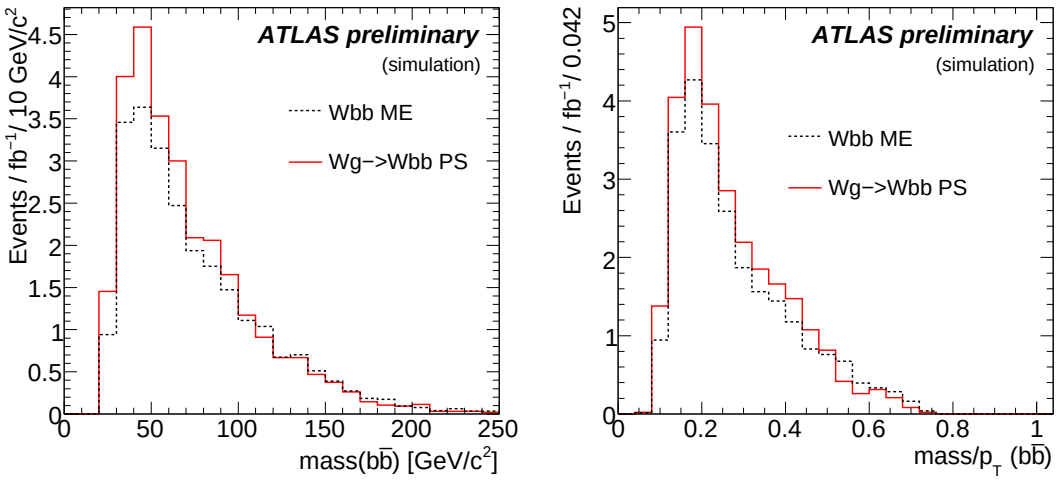

Figure 1: Distributions of the kinematics of the $b\bar{b}$ system in the $Wb\bar{b}$ background comparing HERWIG ($Wg \to$ bb PS) and AcerMC ($Wb\bar{b}$ ME), after selecting $b\bar{b}$ pairs with $p_{\mathrm{T}} > 200$ GeV and $1.3 > \Delta R(b\bar{b}) > 0.3$. The left plot shows the mass distribution for the $b\bar{b}$ pair, the right plot the same quantity divided by its transverse momentum. Both distributions are normalised to their relative cross sections in fb.

2 Event Samples and Detector Simulation

All the event samples were generated with the HERWIG 6.510 Monte Carlo generator [12] using JIMMY 4.31 [13] to simulate the underlying event, assuming a centre-of-mass energy of 14 TeV. An exception is that the AcerMC 3.5 [14] Monte Carlo generator was used to produce single top events, as well as additional $Wb\bar{b}$ samples used as a cross-check. For the $Wb\bar{b}$ sample AcerMC was interfaced to HERWIG for the parton showering and to JIMMY for the underlying event, while for the single-top sample PYTHIA 6.412 [15] was used. For all processes, the CTEQ6L1 (LO) PDFs were used [16]. In the case of the AcerMC processes, the factorization and renormalization scales Q^2 were set for Wt to $\sum_{i=[t,W]} \left({p_{\mathrm{T}}^i}^2 + m_i^2 \right)/2$, while for $W + b\bar{b}$ they were set to $\sum_{i=partons} \left({p_{\mathrm{T}}^i}^2 + m_W^2 \right)/2$.

For the $WH, W \to \mu\nu, e\nu$ analysis the dominant backgrounds are WZ, W+jet, $t\bar{t}$ and single top. For the other analyses, Z+jet dominates, but the remaining backgrounds and the diboson ZZ and WW events are also considered.

The W+jet background, after b-tagging is applied, is dominated by the irreducible $q\bar{q} \to Wg \to Wb\bar{b}$ component. The kinematic region of our analysis, in which a $b\bar{b}$ pair is present at high p_{T}, is such that the leading-logarithmic parton-shower approximation (PS) as implemented in HERWIG (or PYTHIA) can be expected to work well, and this was verified by comparisons with AcerMC, which used the full matrix element (ME) including the effects of b-quark mass, as shown in Fig. 1. The HERWIG samples were used for the baseline result since AcerMC does not include matching to the final-state parton shower, which leads to a depletion of gluon radiation in the kinematic region where most of the background contribution is expected.

All the samples are leading order and/or leading logarithmic, and no K-factors were applied to emulate higher order effects. At the LHC, a large enhancement in the $W + b\bar{b}$ cross section is expected at NLO, essentially because a new process ($qg \to Wb\bar{b}j$), which cannot just be

described with additional initial state radiation, comes into play at NLO (see Ref. [17, 18]): however, in this case an additional hard jet is expected in the event and, due to the jet veto implemented in the analysis, this additional NLO contribution is expected to be highly reduced (see Ref. [19]). In addition, the leading-logarithmic contribution to this correction will again be included in HERWIG.

For the single top background, three different channels have to be considered: s- and t-channel and Wt production. In the hadron level study performed in Ref. [3], it was noticed that the single top s- and t-channels produce a negligible level of background. The s-channel ($qq \to tb$) has a very low cross section (7.1pb at LO), the t channel $gq \oplus qg \to qt \oplus b$ has a large cross section (251pb at LO), but neither process can easily fake the signal topology, where a heavy highly boosted object decaying to a $b\bar{b}$ pair is expected together with a high p_{T} W boson decaying into a lepton on the other side. In fact in these channels one of the two b-jets is either soft, or goes into a direction opposite to the top. Since the other b-jet needs to come from the top, and the top needs to be sufficiently boosted to produce a high p_{T} W boson, this is very unlikely. For this reason no single top events for the s and t-channels were produced in this study. However, the Wt channel needs to be considered, because its topology is close to the signal, with one W on one side and a top on the other side, which fakes the Higgs candidate in case one of the three produced jets from the top is very soft and remains undetected, while the remaining c- and b- quarks fake the $b\bar{b}$ pair. This background was not considered in Ref. [3], and is studied here for the first time for this channel.

A simple parton level study was also performed to make sure the $t\bar{t}Z$ background does not provide a significant background to this analysis.

Finally, no background from QCD multi-jet events was considered. In order to reduce the impact of jets faking leptons, an isolation requirement on muons and electrons is applied (see Sec. 4.2). There is nothing particular in this analysis which would enhance the QCD fake background compared to more normal (low p_{T}) W and Z studies, where such backgrounds are found to be very small [2]. However, the kinematic configuration and flavour composition selected in this analysis is sufficiently different that a more detailed study of such background would be of value. More detailed studies suffer from the extremely high statistics needed for generating such samples. In general, given the high p_{T} cuts adopted in the analysis both for the W and Higgs boson candidates, it should be more difficult for the QCD dijet background to pass through the analysis cuts than in more inclusive analyses.

To produce the large number of events needed for this study, all signal and background samples were passed through the AtlFast-II simulation, which corresponds to a full simulation of the ATLAS inner detector and muon system and a fast simulation of the calorimeter in its full granularity relying on the FastCaloSim package [20]. The WH signal sample at a reference mass of 120 GeV was also passed through the full simulation of the ATLAS Detector, in order to cross-check how well the fast simulation of the calorimeter can reproduce the key variables in this analysis (especially the subjet variables). While the fast simulation correctly reproduces the differential distributions which are most relevant for the analysis, e.g. the Higgs invariant mass distribution, it overestimates the reconstruction efficiency of the $H \to b\bar{b}$ system by ≈ 5 % with respect to full simulation: this discrepancy has not been corrected for in the present analysis.

3 Higgs Candidate Identification

When a fast-moving Higgs boson decays, we reconstruct a single fat jet containing two b quarks. The identification strategy proposed in Ref. [3] uses the inclusive, longitudinally invariant C/A

algorithm to flexibly adapt to the fact that the $b\bar{b}$ angular separation varies significantly with the Higgs p_{T} and decay orientation. In this algorithm the angular distance $\Delta R_{ij}^2 = (y_i - y_j)^2 + (\phi_i - \phi_j)^2$, where y is the pseudorapidity and ϕ the azimuthal angle, is calculated between all pairs of objects i and j. The closest pair is combined into a single object, the set of distances is updated, and the procedure is repeated until all objects are separated by a $\Delta R_{ij} > R$, where R is a parameter of the algorithm. This provides a hierarchical structure for the clustering, like the $k_\perp$ algorithm but in angles rather than in relative transverse momenta. It is implementated in FastJet 2.3 [21] and interfaced to the ATLAS core software in Athena. The jet finder is applied to topolological clusters identified in the ATLAS calorimeter, and cell-by-cell and local hadron calibrations [2, 22] are applied: at any stage of the jet clustering algorithm, the jet mass, m, is defined summing up the four momenta of all constituents considered for the clustering. The three-dimensional clusters of energy reconstructed in the calorimeter and used as basic input for the jet clustering algorithm are treated as massless. All jets j corresponding to the history stage at $\Delta R_{ij} = 1.2$, that is the stage at which all jets are separated from each other by at least $\Delta R = 1.2$, are selected. Those jets with $p_{\mathrm{T}} > 200$ GeV and $|\eta| < 2.5$ are subjected to an iterative decomposition procedure involving two dimensionless parameters, μ and y_{cut}. A full explanation of the procedure can be found in Ref. [3], and we directly quote the main stages below:

1. Break the jet j into two subjets by undoing its last stage of clustering. Label the two subjets j_1, j_2 such that $m_{j_1} > m_{j_2}$.

2. If there was a significant mass drop (MD), $m_{j_1} < \mu m_j$, and the splitting is not too asymmetric, $y = \frac{\min(p_{tj_1}^2, p_{tj_2}^2)}{m_j^2} \Delta R_{j_1,j_2}^2 > y_{\mathrm{cut}}$, then deem j to be the heavy-particle neighbourhood and exit the loop. Note that $y \simeq \min(p_{tj_1}, p_{tj_2}) / \max(p_{tj_1}, p_{tj_2})$.

3. Otherwise redefine j to be equal to j_1 and go back to step 1.

In the above quoted list, the "heavy-particle neighbourhood" is the region to which angle-ordered QCD radiation from the Higgs decay products is expected to be confined. The two parameters μ and y_{cut} may be chosen independently of the Higgs mass and of p_{T}. We use $\mu = 1/\sqrt{3}$, which ensures that if, in its rest frame, the Higgs decays in such a way that the energy is equally shared between the three partons in a $b\bar{b}g$ configuration, then it will still trigger the mass drop condition. The cut on $y \simeq \min(z_{j_1}, z_{j_2}) / \max(z_{j_1}, z_{j_2})$, where z_{j_1} and z_{j_2} are the momentum fractions of the two quarks, eliminates the asymmetric configurations that most commonly generate significant jet masses in non-b or single-b jets because of the high probability of soft gluon radiation. We apply a cut at $y_{cut} = 0.1$. The analysis is not strongly sensitive to the exact values chosen for these parameters, as illustrated in Fig. 2, where the mass distribution for Higgs candidates in a signal sample is shown for various values of y_{cut}. In addition, also the distribution of the y parameter values of the clustered Higgs candidates after analysis selection cuts is shown in Fig. 2 for the signal and various backgrounds in the $l\nu b\bar{b}$ channel.

The angular distance between j_1 and j_2, $R_{b\bar{b}}$, defines the distance between the two b-quarks. In order to obtain good b-tagging performance, a reliable separation and reconstruction of the two b-subjets is needed, so that the direction of the two b-subjets can be considered as a reasonable approximation for the direction of the outgoing b-partons after eventual QCD final state radiation. This is crucial in order to correctly associate to the two subjets their charged-particle tracks as reconstructed in the inner detector, avoiding to a large extent cross-talk between the two subjets. As a consequence the jet clustering procedure has to be optimized not only to provide a good invariant mass resolution for the Higgs candidate, but also to provide a good

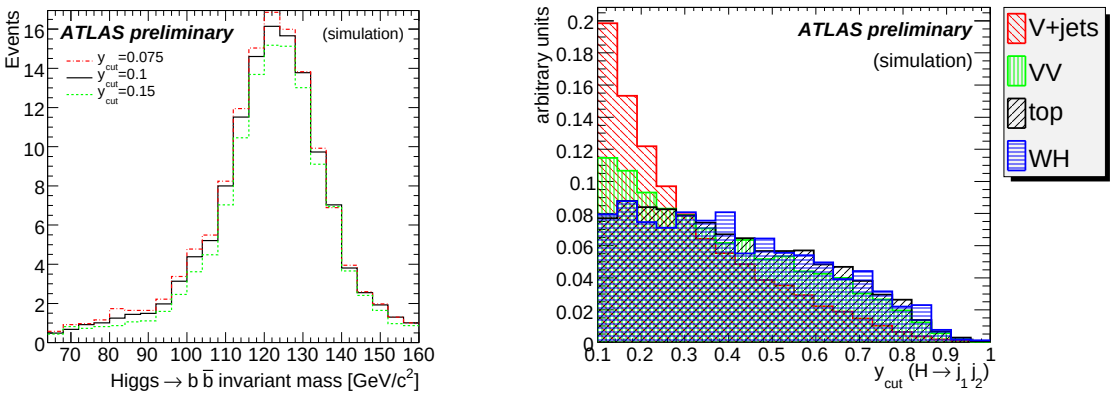

Figure 2: (Left) Invariant mass distribution of the Higgs candidates in the WH signal sample for various values of the y_{cut} clustering parameter, before application of b-tagging and jet vetoes. Numbers are projected to an integrated luminosity of 30 fb^{-1}. (Right) Distribution of the y parameter values for the signal and various backgrounds in the $l\nu b\bar{b}$ channel, after the analysis selection is applied, except for the b-tagging requirement. The histograms are normalized to an area of 1.

angular resolution on the direction of the two subjets and to try to select the $b\bar{b}$ pair out of a $b\bar{b}g$ configuration.

At this stage, the effective size of jet j will be just sufficient to contain the QCD radiation from the Higgs decay, which, because of angular ordering [23–25], will be almost entirely emitted in the two angular cones of size $R_{b\bar{b}}$ around the b quarks. Since this radius sets the angular scale (candidate-by-candidate) of the Higgs decay, it makes sense to recluster, or *filter* the candidate using this information. This involves rerunning the C/A algorithm on the jet constituents, using a finer angular scale, $R_{\rm filt} < R_{b\bar{b}}$, and taking the three hardest objects (sub-jets) that appear — thus one captures the dominant $\mathcal{O}(\alpha_s)$ radiation from the Higgs decay, while eliminating much of the contamination from the underlying event. We follow Ref. [3] in using $R_{\rm filt} = \min(0.3, R_{b\bar{b}}/2)$. The jet j is accepted as a Higgs candidate if the two hardest subjets have b tags. The filtering procedure provides also an effective way to remove some of the contributions arising directly from the showering of the b-quark before hadronisation (i.e. no long-lifetime component) and thus improves the angular resolution of the two hardest subjets with respect to the two b-hadrons arising from the b-quark pair, which is a fundamental ingredient for b-tagging.

The identification of the two b-quarks originating from the Higgs boson is crucial for separating the signal from the large backgrounds. The b-tagging algorithms used in this analysis combine impact parameter information with the explicit determination of an inclusive secondary vertex, providing the highest b-tagging performance available within ATLAS [2]. To apply b-tagging, tracks are assigned to subjets if their direction at the vertex is within $\Delta R = 0.4$ of the subjet direction as determined by the jet clustering algorithm. Every track is assigned to at most one subjet, so in case of overlaps a track is assigned to the nearest in ΔR of the two subjets.

The rejection achievable against light- and c-quark jets was analyzed in the specific kinematic configuration and using the signal and background samples relevant for this analysis and is shown in Fig. 3 as a function of the b-tagging efficiency on the b-subjet. At 70 % b-tagging efficiency (corresponding to $\approx 50\%$ signal efficiency), a rejection of light quark jets around 100

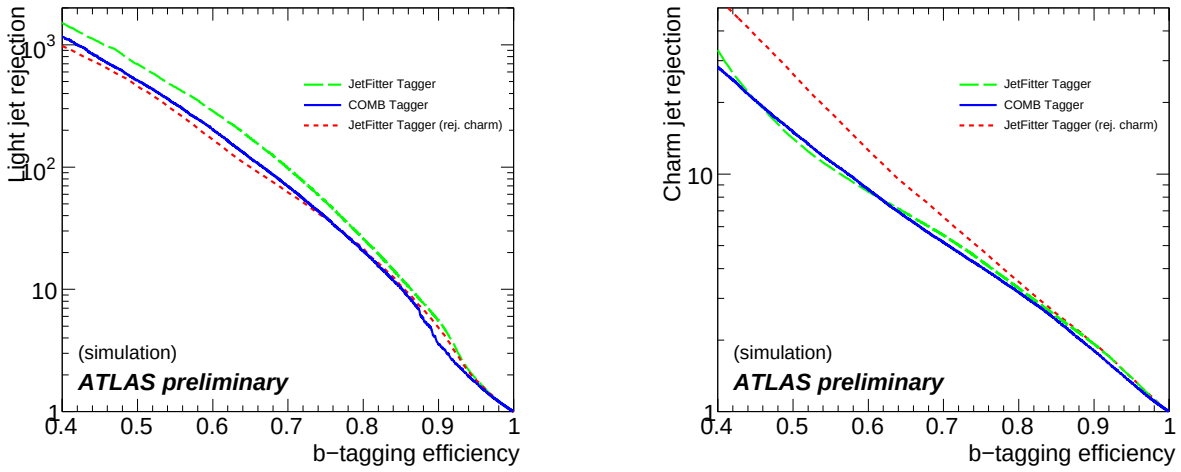

Figure 3: Rejection against light-quark jets (left) and against charm-quark jets (right) as a function of the b-tagging efficiency on the single subjet, for both the COMB and JetFitter b-tagging algorithms. The performance for the JetFitter algorithm is also shown after dedicated optimization to reject c-jets.

is expected to be achievable, corresponding to 1% light-jet misidentification efficiency. This is exactly the value considered in the generator level study [3] in the most optimistic scenario. Such an efficient rejection of the background is however only valid in the hypothesis that the background is dominated by light-jets, so that charm-jets do not play an important role.

Since charm-quarks fragment into c-hadrons which possess a significant lifetime and have similar decay multiplicities to b-hadrons, separating b-jets from c-jets is much harder than separating b-jets from light jets, as shown in the right plot in Fig. 3. To improve the rejection against charm-jets, a dedicated b-tagging algorithm is used, JetFitter [26], which provides extra information, trying for example to identify the $PV \rightarrow b \rightarrow c$ decay chain topology, which is not present in a c-jet. Two discriminating variables are used, one trained against light jets, the second against c-jets: they are combined by reweighting them respectively according to the prior light (c(light)) and c-jet (1 − c(light)) relative flavour composition of the background, at the cost of a reduced light-jet rejection. The value for c(light) has been optimized by scanning the 0-1 range using 0.2 intervals[1)].

While b-tagging can easily reduce the number of b-light subjet combinations to an acceptable level, it is much harder to reduce the b-c component, which most often occurs in the $t\bar{t}$ backgrounds. In W+jets the dominant contribution comes from the light-light and light-c subjet combinations, as expected from pure QCD production. The most dangerous contribution comes however from $b\bar{b}$ pairs (e.g. from gluon splitting), which cannot be reduced by applying b-tagging.

To determine the optimal b-tagging strategy for the present analysis, the significance, defined as $\frac{S}{\sqrt{B}}$ has been analyzed as a function of the signal efficiency given for a certain b-tagging requirement, for the $l\nu b\bar{b}$ channel. This is shown in Fig. 4.

[1)]Since the b-tagging algorithm was not specifically optimized and trained in the kinematic and topological region of the present analysis, the prior light jet composition factor c(light) does not necessarily reflect the real flavour composition of the background.

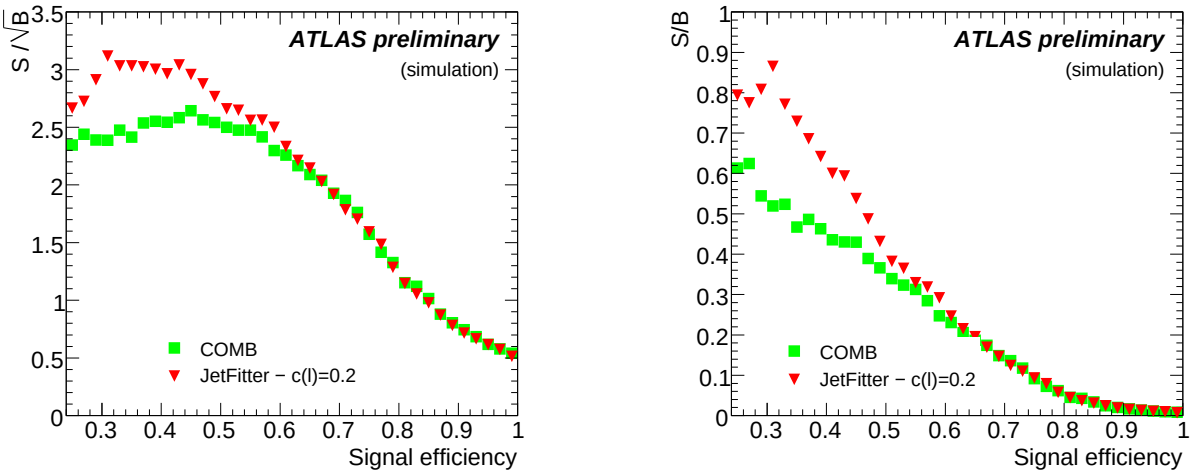

Figure 4: Statistical significance (left) and signal over background ratio (right) after 30 fb^{-1} for the $l\nu b\bar{b}$ channel as a function of the signal efficiency corresponding to a certain b-tagging cut, using either the ATLAS default combined b-tagging algorithm or the JetFitter algorithm tuned with a prior background light-jet content of 20%.

The tagger provides a relatively flat significance between $\approx 35-45\%$ signal efficiency. A working point at 40% signal efficiency was chosen.

After the Higgs candidate has been identified and tagged as described above, a cut at $p_{\mathrm{T}} > 200\,\mathrm{GeV}$ is applied to the momentum of the filtered Higgs candidate. The filtered four-momentum, computed from the three highest p_{T} filtered subjets, is considered in all subsequent steps.

4 Analysis

4.1 Trigger Selection

Trigger efficiencies have been studied in fully-simulated samples. The analyses for the $l\nu b\bar{b}$ and $llb\bar{b}$ channels make use of muons and electrons with $p_{\mathrm{T}} > 25 \sim 30\,\mathrm{GeV}$. These leptons are of sufficiently high transverse momenta for triggering most events for instantaneous luminosities up to $2{\times}10^{33}$ cm^{-2} s^{-1} [2]. Losses are expected due to the geometrical acceptance of the muon and electron trigger systems. However, in the case of muons, these can be recovered by making use of jet and $E_{\mathrm{T}}^{\mathrm{miss}}$-based triggers. While most jet triggers are expected to be heavily prescaled up to very high momenta, a jet AND $E_{\mathrm{T}}^{\mathrm{miss}}$ combination trigger with relatively low thresholds is expected to be among those that will be unprescaled at $2{\times}10^{33}$ cm^{-2} s^{-1} [2]. This signature is interesting not only when a genuine $E_{\mathrm{T}}^{\mathrm{miss}}$ signature is present, but also when we lose muons due to Level 1 trigger acceptance, creating fake missing momentum.

As expected, $e^+e^-b\bar{b}$ has a high trigger efficiency of $(98.6 \pm 0.6)\%$ for the lepton triggers. Combining lepton triggers with the $E_{\mathrm{T}}^{\mathrm{miss}}$·jet trigger, an overall trigger efficiency of $(99.4 \pm 0.2)\%$ is obtained for our offline selected events in the $l\nu b\bar{b}$ channel. For the $\mu^+\mu^-b\bar{b}$ events it is $(99.8 \pm 0.2)\%$. Finally, the $E_{\mathrm{T}}^{\mathrm{miss}}b\bar{b}$ channel does not benefit from the lepton triggers at all, but the large missing energy can be triggered on, with the threshold at high luminosity likely to be around $100-125\,\mathrm{GeV}$. Therefore events with $E_{\mathrm{T}}^{\mathrm{miss}} > 200\,\mathrm{GeV}$ have an expected overall effiency

of $(97.2 \pm 0.4)\%$.

The conclusion is that, due to the presence of high-p_{T} leptons and/or high $E_{\mathrm{T}}^{\mathrm{miss}}$, no significant loss is expected at the trigger for events from any of the channels studied.

4.2 $l\nu b\bar{b}$ channel

The selection procedure relies on the following criteria:

- Highest p_{T} muon or electron with $p_{\mathrm{T}} > 30$ GeV
- $E_{\mathrm{T}}^{\mathrm{miss}} > 30\,\mathrm{GeV}$, consistent with a W boson with $p_{\mathrm{T}} > 200$ GeV
- H candidate with $p_{\mathrm{T}} > 200\,\mathrm{GeV}$ and $|\eta| < 2.5$
- Z and H candidates not within 1.2 radians of each other in ϕ
- Veto on additional electrons or muons in the event with $p_{\mathrm{T}} > 10$ GeV.
- Veto on additional b-tagged jets with $p_{\mathrm{T}} > 15$ GeV
- Veto on additional jets with $p_{\mathrm{T}} > 20$ GeV and $|\eta| < 5$
- The two leading subjets of the H candidate pass the b-tagging requirement.

A loose isolation requirement is applied on the highest p_{T} lepton in the event, to reject eventual background from QCD events. In case of a muon it is required that:

$$\frac{E_{T,cone}}{E_t(\mu)} < 25\%,$$

where $E_{T,cone}$ is the amount of transverse energy in the calorimeter in a cone of $\Delta R = 0.4$ around the track, as extrapolated to the calorimeter entrance. In the case of an electron the isolation requirement is:

$$\frac{E_{T,cone}(\Delta R = 0.2)}{p_{\mathrm{T}}(e)} < 10\%.$$

The dominant backgrounds are WZ, W+jets, $t\bar{t}$ and Wt. The signal and the di-boson WZ background can only be distinguished due to their different di-jet invariant mass: the mass window cut reduces this background contribution to a small level, but a good invariant mass resolution is a crucial ingredient to obtain such a suppression. The W+jets background is strongly reduced by the requirement of two b-tagged subjets, so the remaining background is dominated by the irreducible $W+b\bar{b}$ contribution. The case of $t\bar{t}$ and Wt is more complex, since the presence of b and c quarks in the final state makes b-tagging less powerful in rejecting this background; however, in particular for $t\bar{t}$, vetoing additional b-jets and the remaining well identified light-jets in the event down to a certain p_{T} can suppress a good part of this contribution.

The expected number of events for signal and the various backgrounds after 30 fb^{-1} of collected data is listed in Table 1. The mass distribution of the Higgs candidates is shown in Fig. 5a. Both Higgs and Z boson peaks are visible on top of the $t\bar{t}$, Wt and W+jets backgrounds, which are dominated by the irreducible $W + b\bar{b}$ contribution. The Wt and $t\bar{t}$ backgrounds are labeled as *top* background in the plots.

The resulting statistical significance, considering the mass range 112-136 GeV, in terms of $\frac{S}{\sqrt{B}}$ is 3.0 ± 0.3, where the quoted uncertainty comes from the limited available Monte Carlo statistics, and the signal to background ratio is $\frac{S}{B} \simeq \frac{2}{3}$. This number can be approximately

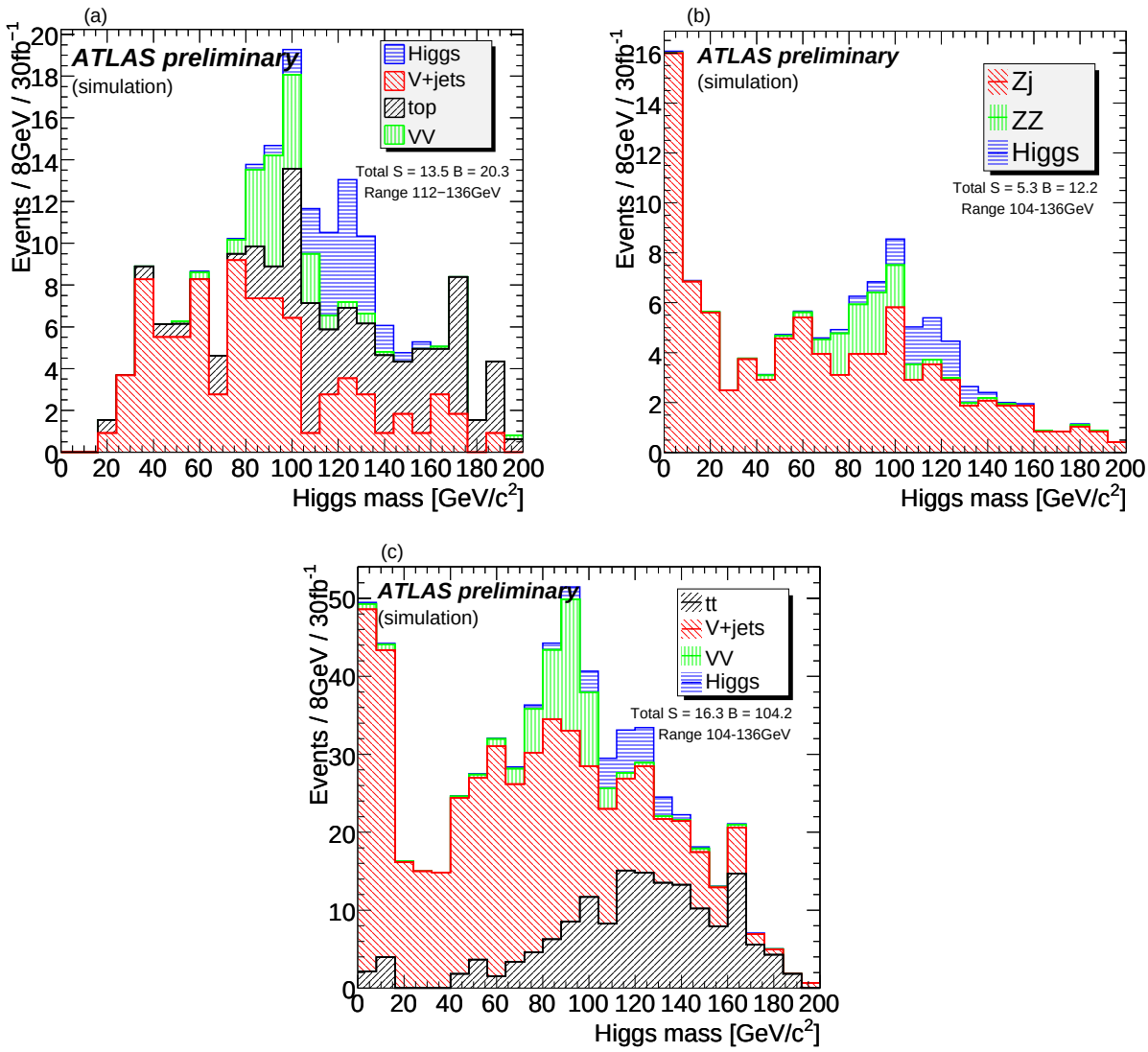

Figure 5: Distribution of the invariant mass of the Higgs candidate after all selection cuts. (a) $l\nu b\bar{b}$ channel (b) $llb\bar{b}$ channel and (c) $E_{\mathrm{T}}^{\mathrm{miss}}b\bar{b}$ channel. The signals (for $m_H = 120$ GeV) are shown on top of the backgrounds. All distributions are normalized to an integrated luminosity of 30 fb^{-1}.

compared to the particle-level result for this channel in Ref. [3] of 3.1. Note that in the particle-level study, high $E_{\mathrm{T}}^{\mathrm{miss}}$ events were in fact counted in the $E_{\mathrm{T}}^{\mathrm{miss}}b\bar{b}$ channel regardless of whether a lepton was identified, thus reducing the relative contribution to the significance from the $l\nu b\bar{b}$ channel compared to our result.

The trigger efficiency has not been applied.

4.3 $llb\bar{b}$ channel

The requirement of leptonic Z decay leads to small branching ratios. However this is counteracted by the fact that it is hard for backgrounds such as $t\bar{t}$ to emulate this signature. The selection consists of two parts, firstly a candidate for the hadronic $H \to b\bar{b}$ system is identified

Before mass window cut						
	WH/ZH	$WW/ZZ/WZ$	$t\bar{t}$	Wt	W+jets	Z+jets
$l\nu b\bar{b}$	19.5 ± 1.0	18.8 ± 1.8	40.4 ± 5.1	18.2 ± 2.4	87.3 ± 9	3.9 ± 1.7
$llb\bar{b}$	8.0 ± 0.4	10.4 ± 0.6	-	-	-	91 ± 4
$E_{\mathrm{T}}^{\mathrm{miss}}b\bar{b}$	24.0 ± 0.6	51.2 ± 5.6	129 ± 11	32 ± 3	127 ± 11	279 ± 14
After mass window cut						
	WH/ZH	$WW/ZZ/WZ$	$t\bar{t}$	Wt	W+jets	Z+jets
$l\nu b\bar{b}$	13.5 ± 0.8	1.4 ± 0.5	5.6 ± 2.4	4.2 ± 1.1	8.3 ± 2.8	0.8 ± 0.8
$llb\bar{b}$	5.3 ± 0.3	1.0 ± 0.2	-	-	-	11 ± 2
$E_{\mathrm{T}}^{\mathrm{miss}}b\bar{b}$	16.3 ± 0.4	4.1 ± 0.7	41 ± 6	11 ± 2	17 ± 4	32 ± 5

Table 1: Expected number of events with 30 fb^{-1} of integrated luminosity after full analysis selection (before and after mass window cut), based on LO cross sections, for all three channels and for all signal and background processes considered.

according to the procedure described in Section 3. A candidate for a leptonic Z is then defined as a pair of opposite sign, same flavour electrons or muons with an invariant mass such that $80 < M_{\ell^+\ell^-} < 100\,\mathrm{GeV}$ where the highest p_{T} of the two leptons satisfies $p_{\mathrm{T}} > 25\,\mathrm{GeV}$ and the other satisfies $p_{\mathrm{T}} > 20\,\mathrm{GeV}$. The selection specific to this channel is:

- H candidate with $p_{\mathrm{T}} > 200\,\mathrm{GeV}$ and $|\eta| < 2.5$
- Z candidate with $p_{\mathrm{T}} > 180\,\mathrm{GeV}$
- Z and H candidates not within 1.2 radians of each other in ϕ
- The two leading subjets of the H candidate pass the b-tagging requirement.

No lepton isolation requirement was applied. Applying this selection we find $t\bar{t}$ production to be a negligible background in this channel.

The mass distribution of H candidates in all samples is shown in Figure 5b, while the expected number of events after 30 fb^{-1} of collected data is listed in Table 1. As in the previous channel, both Higgs and Z boson peaks are visible on top of the background, which in this case is dominated by Z+ jets. The resulting statistical significance in terms of $\frac{S}{\sqrt{B}}$ is 1.5 ± 0.2, where the quoted uncertainty comes from the limited available Monte Carlo statistics, and the signal to background ratio is $\frac{S}{B} \simeq \frac{1}{3}$.

The effect of trigger efficiency is not included. This number can be compared to the particle-level result for this channel in [3] of 2.1.

4.4 $E_{\mathrm{T}}^{\mathrm{miss}}b\bar{b}$ channel

Events where a $H \to b\bar{b}$ system is produced in association with a large amount of missing E_{T} come primarily from the process $ZH \to \nu\bar{\nu}b\bar{b}$. There is also a contribution from $WH \to l\nu b\bar{b}$ where the charged lepton has not been correctly identified and therefore a W cannot be reconstructed in the $l\nu b\bar{b}$ analysis. This channel offers greater signal cross-sections than the $llb\bar{b}$ channel but does not have the strong background rejection provided by the $Z \to ll$ decay.

The $H \to b\bar{b}$ identification is again as defined in Section 3. The requirement of no leptons ensures that the sample of events selected in this channel is independent of that extracted in the $l\nu b\bar{b}$ channel in Section 4.2. The selection for this channel is as follows:

- H candidate with $p_{\mathrm{T}} > 200\,\mathrm{GeV}$ and $|\eta| < 2.5$
- $E_{\mathrm{T}}^{\mathrm{miss}} > 200\,\mathrm{GeV}$
- No electron or muon with $p_{\mathrm{T}} > 30\,\mathrm{GeV}$
- Jet veto: no additional jet with $p_{\mathrm{T}} > 30\,\mathrm{GeV}$
- H candidate and $E_{\mathrm{T}}^{\mathrm{miss}}$ are not within 1.2 radians of each other in ϕ
- The two leading subjets of the H candidate pass the b-tagging requirement.

After applying this selection the final mass distribution of H candidates can be found in Fig. 5c, while the expected number of events after 30 fb^{-1} of data is listed in Table 1. The final statistical significance in terms of $\frac{S}{\sqrt{B}}$ after applying this selection is 1.6 ± 0.1 for 30 fb^{-1} of luminosity, where the quoted uncertainty comes from the limited available Monte Carlo statistics. This number can be approximately compared to the particle-level result for this channel in [3] of 3.1, however, as already explained, in the hadron level study some of the $l\nu b\bar{b}$ events were considered as belonging to the $E_{\mathrm{T}}^{\mathrm{miss}}$ channel, increasing the relative contribution to the significance from the $E_{\mathrm{T}}^{\mathrm{miss}}$ channel compared to our result.

5 Combination of channels

The results of the analyses are combined to evaluate an overall significance. A profile likelihood method is applied, according to the general procedure used in the Higgs chapter of Ref. [2]. Assuming simple event counting experiments, the likelihood function for a given experiment i where n events are observed is Poisson:

$$L_i(\mu) = \frac{(\mu s_i + b_i)^{n_i}}{n_i!} e^{-(\mu s_i + b_i)}, \tag{1}$$

where b and s represent expected background and signal levels respectively. The symbol μ parameterises the level of signal present, $\mu = 1$ representing the standard model case. Since we are combining several analyses, the form of a combined likelihood function is required. The likelihood function for N experiments of the type described above can be expressed as:

$$L(\mu) = \prod_{i=1}^{N} L_i(\mu) \tag{2}$$

The test statistics is then defined as:

$$q(0) = -2\ln(\lambda(0)) \tag{3}$$

where $\lambda(0)$ is the value of the profile likelihood ratio, obtained dividing the likelihood maximized with μ constrained to be zero by the same likelihood maximized with μ left floating:

$$\lambda(0) = \frac{L(\mu = 0)}{L(\hat{\mu})}. \tag{4}$$

We also include an estimate of the effects of systematic uncertainties. The dominant experimental uncertainties are estimated to come from shifts in the jet energy scale, variations in the invariant mass resolution, differences in the b-tagging efficiency and rejection factors in data

with respect to simulation. In the presence of backgrounds peaking in the vicinity of the signal region (Fig. 5), it is reasonable to assume that the dominant systematic uncertainties will result from the imperfect understanding of these backgrounds.

The backgrounds of the separate channels are neither fully correlated nor completely independent. To reflect this, we break the backgrounds into three groups, which are independent of each other but completely correlated between the separate channels. The 3 groups are:

- $t\bar{t}$, WW, WZ and ZZ
- $W + jets$ and Wt
- $Z + jets$.

Their background levels are defined respectively as t_i, w_i and z_i, where the index i refers to the channels considered, and a common Gaussian uncertainty on the expectation value of each background type is then assumed. This is modelled in the likelihood formalism by adding common nuisance parameters C_t,C_w,C_z to the combined likelihood function:

$$\begin{aligned} L(\mu, C_t, C_w, C_z) &= \prod_{i=1}^{N} \frac{(\mu s_i + C_t t_i + C_w w_i + C_z z_i)^{n_i}}{n_i!} e^{-(\mu s_i + C_t t_i + C_w w_i + C_z z_i)} \times \\ & \quad Gaus(C_t) \times Gaus(C_w) \times Gaus(C_z), \end{aligned}$$

where:

$$Gaus(C_x) = \frac{1}{\sigma_x \sqrt{2\pi}} e^{-\frac{(C_x - 1)^2}{2\sigma_x^2}}.$$

In a more complete treatment there would be many partially correlated uncertainties on the background level due to factors such as luminosity, cross-section and detector efficiency. Splitting the background into three completely uncorrelated uncertainties should provide enough degrees of freedom to give a rough but reasonable estimate of how this uncertainty affects the final significance.

Using as input the signal and background expectation values, the values for which are given in Table 2, a large number ($> 10,000$) of background only pseudoexperiments was generated to get the distribution of p-values (that is the fraction of experiments at least as unlikely as the current one) as a function of the test statistics $q(0)$. Then many experiments containing also the signal were generated and according to their $q(0)$ value their significance was calculated, as shown in Fig. 6. Out of the distribution of possible outcomes, the median is taken as a reasonable expectation of performance. We are using the combination for our three channels: $llb\bar{b}$, $l\nu b\bar{b}$ and $\nu\nu b\bar{b}$. Initially, a perfect understanding of the backgrounds is assumed and the results are as seen in Fig. 6. Here a median significance of $3.7^{+0.3}_{-0.2}\sigma$ is observed, which is consistent with the expectation from adding the $S/\sqrt{B}$ significances in quadrature. The error shown here is associated with the limited Monte Carlo statistics.

A variety of possible background uncertainties are then tested, the results of which can be found in Table 3.

The exact background uncertainties for each channel depend on the mixture of different background samples. A 10% uncertainty in each of the three background samples corresponds to a 9%, 7% and 6% uncertainty on the total background level in the $llb\bar{b}$, $l\nu b\bar{b}$ and $\nu\nu b\bar{b}$ channels

Channel	signal	t_i	w_i	z_i	$S/\sqrt{B}$
$llb\bar{b}$	5.34	0.98	0.0	11.2	1.5
$l\nu b\bar{b}$	13.5	7.02	12.5	0.78	3.0
$\nu\nu b\bar{b}$	16.3	45.2	27.4	31.6	1.6
Combined					3.7

Table 2: Expected number of events after 30 fb^{-1} of integrated luminosity for each channel, subdivided into the signal or background classes defined for the combination in the text.

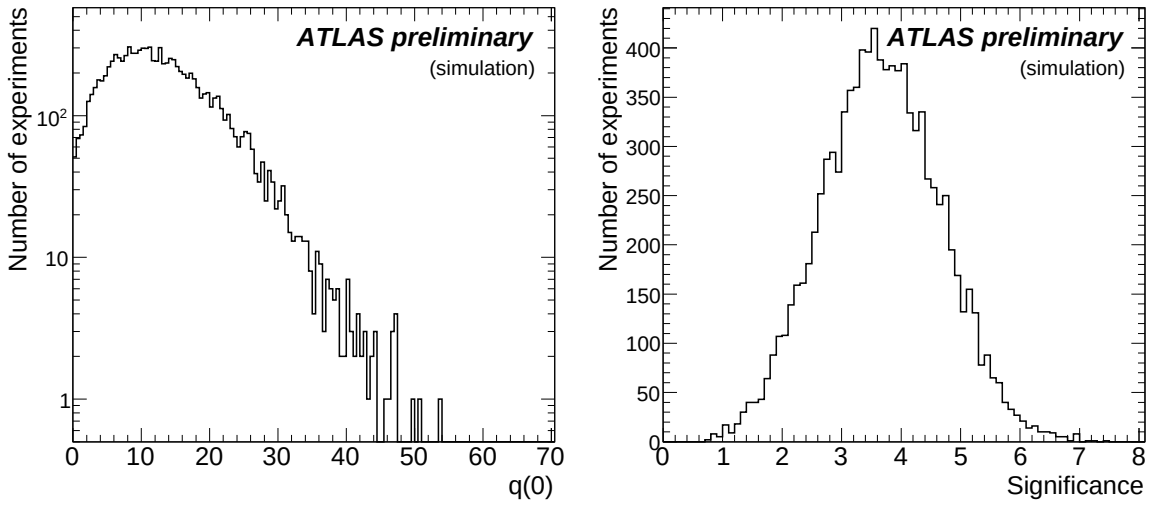

Figure 6: $q(0)$ and significance for a range of possible signal experiments.

respectively. These numbers scale linearly with sample uncertainty. Given that after 30 fb^{-1} of data ATLAS should also have strong understanding of the background from other sources we estimate that an uncertainty of 10% or better is realistic.

The significance of 3.7σ in the perfect case is found to be reduced to 3.2σ in the case of a 10% uncertainty and 3.0σ in the case of a 15% uncertainty on the expected level of each background sample. It is useful to note that the combination of the three separate channels with differing background compositions helps reduce the effects of this systematic uncertainty.

6 Summary and Outlook

We have presented a first study of the ATLAS sensitivity to the HZ and HW associated production channels at high-p_{T} for a low-mass Standard Model Higgs boson using a realistic detector simulation, based on a full Geant4 simulation of the detector response in the inner detector and muon system and on a fast simulation of the calorimeter response in its full granularity. The analysis closely follows that of Ref. [3], but uses a realistic simulation of the ATLAS detector and trigger, and the full ATLAS reconstruction software. The trigger efficiencies are found to be very high for all channels considered. The signal selection efficiency in the $l\nu b\bar{b}$ channel agrees with a full Geant4 simulation of the whole ATLAS detector within ≈ 7 %, while such a direct comparison was not evaluated for the background samples. All the expected significant back-

σ_t	σ_w	σ_z	Significance
Perfect	Perfect	Perfect	3.7
5%	5%	5%	3.5
10%	10%	10%	3.2
15%	15%	15%	3.0
20%	20%	20%	2.8
30%	30%	30%	2.5
50%	50%	50%	2.2
75%	75%	50%	2.0
50%	10%	10%	2.8

Table 3: Significances for different scenarios with differing background uncertainties after 30 fb^{-1}.

grounds are studied, including that from Wt, which was not considered in Ref. [3]. Sensitivities are given as a function of the eventual systematic uncertainty in the background.

For the cut-based analysis presented here, the combined sensitivity of these channels after an integrated luminosity $L = 30$ fb^{-1} of data, considering only statistical errors, is 3.7σ for a Higgs-boson mass of 120 GeV. If the major backgrounds have a systematic uncertainty of around 15%, the significance drops to 3.0σ, and if the systematic uncertainty is as high as 50% this sensitivity drops to around 2.2σ. For $L = 10$ fb^{-1} we might expect sensitivity of up to 2.1σ. This is very close to the ATLAS sensitivity in any other single channel [2] in this region. In addition, this channel would give the most direct information on the $H \to b\bar{b}$ coupling and will therefore be critical for determining the parameters of the Higgs sector [27].

All numbers are based on signal and background processes generated at LO and normalized to their respective LO cross sections. While a first evaluation of the impact of the NLO estimate of their cross sections was made in Ref. [3] at parton level and the impact on the significances found to be small, the use of dedicated NLO generators, whenever possible, is foreseen for a future update of the analysis.

Further improvements can be expected in this analysis. The b-tagging might be calibrated and further optimized for this specific kinematic region, aiming at a higher b-tagging efficiency while preserving a similar light and charm-jet rejection. The jet calibrations could be redone for these specific jets, hopefully improving the mass resolution. Perhaps most importantly, the background can be extracted directly from the data. Finally, the use of signal and background shape information and sophisticated multivariate techniques similar to those currently being applied at the Tevatron should enhance the sensitivity compared to the relatively simple cut-based analysis presented here.

The simulation of pile-up and of cavern background was not considered in the present study: while a preliminary study shows that the impact of pile-up (at an instantanous luminosity of $2{\times}10^{33}$ cm^{-2} s^{-1}with nominal bunch crossing time of 25 ns) on the subjet reconstruction efficiency and on the Higgs invariant mass resolution is small, more studies are needed to fully understand the impact on the b-tagging performance and in particular on the jet veto efficiency, which seems to be substantially degraded by pile-up if no additional corrections are applied.

In conclusion, we have confirmed with a realistic detector simulation that by studying the high-p_{T} regions and employing state-of-the-art subjet techniques, the HZ and HW channels can be reinstated as one of the promising search and measurement channels for the low-mass Standard Model Higgs at ATLAS.

References

[1] T. Gadfort and S. Griso, presented at Moriond QCD and High Energy Interactions March 14th - March 21st 2009.

[2] The ATLAS Collaboration, G. Aad *et al.*, arXiv:0901.0512.

[3] J. M. Butterworth, A. R. Davison, M. Rubin and G. P. Salam, Phys. Rev. Lett. **100**, 242001 (2008), [0802.2470].

[4] S. Catani, Y. L. Dokshitzer, M. H. Seymour and B. R. Webber, Nucl. Phys. **B406**, 187 (1993).

[5] S. D. Ellis and D. E. Soper, Phys. Rev. **D48**, 3160 (1993), [hep-ph/9305266].

[6] J. M. Butterworth, B. E. Cox and J. R. Forshaw, Phys. Rev. D **65** (2002), [hep-ph/0201098].

[7] Reconstruction of high mass $t\bar{t}$ resonances in the lepton+jets channel, ATL-PHYS-PUB-2009-081.

[8] Discovering heavy particles decaying into single boosted jets with substructure using the $k_\perp$ algorithm, ATL-PHYS-PUB-2009-076.

[9] ATLAS Collaboration, G. Aad *et al.*, JINST **3**, S08003 (2008).

[10] Y. L. Dokshitzer, G. D. Leder, S. Moretti and B. R. Webber, JHEP **08**, 001 (1997), [hep-ph/9707323].

[11] M. Wobisch and T. Wengler, hep-ph/9907280.

[12] G. Corcella *et al.*, hep-ph/0210213.

G. Corcella *et al.*, JHEP **01**, 010 (2001), [hep-ph/0011363].

[13] J. M. Butterworth, J. R. Forshaw and M. H. Seymour, Z. Phys. **C72**, 637 (1996), [hep-ph/9601371].

[14] B. P. Kersevan and E. Richter-Was, hep-ph/0405247.

[15] T. Sjostrand, S. Mrenna and P. Skands, JHEP **05**, 026 (2006), [hep-ph/0603175].

[16] J. Pumplin *et al.*, JHEP **07**, 012 (2002), [hep-ph/0201195].

[17] R. K. Ellis and S. Veseli, Phys. Rev. **D60**, 011501 (1999), [hep-ph/9810489].

[18] F. Febres Cordero, L. Reina and D. Wackeroth, Phys. Rev. **D78**, 074014 (2008), [0806.0808].

[19] J. Campbell, R. K. Ellis and D. L. Rainwater, Phys. Rev. **D68**, 094021 (2003), [hep-ph/0308195].

[20] ATLAS Collaboration, G. Aad *et al.*, Simulation of the ATLAS detector, paper in preparation.

[21] M. Cacciari and G. P. Salam, Phys. Lett. **B641**, 57 (2006), [hep-ph/0512210].

[22] H1 Collaboration, I. Abt *et al.*, Nucl. Instrum. Meth. **A386**, 348 (1997).

[23] A. H. Mueller, Phys. Lett. **B104**, 161 (1981).

[24] B. I. Ermolaev and V. S. Fadin, JETP Lett. **33**, 269 (1981).

[25] A. Bassetto, M. Ciafaloni and G. Marchesini, Phys. Rept. **100**, 201 (1983).

[26] G. Piacquadio and C. Weiser, J. Phys. Conf. Ser. **119**, 032032 (2008).

[27] R. Lafaye, T. Plehn, M. Rauch, D. Zerwas and M. Duehrssen, arXiv:0904.3866 [hep-ph].